

Influence of Raman crystallinity on the performance of micromorph thin film silicon solar cells

Ch. Ellert^{a,*}, C. Wachtendorf^b, A. Hedler^b, M. Klindworth^a, M. Martinek^a

^a OC Oerlikon Solar Ltd., Trübbach, Hauptstrasse 1a, CH-9477 Trübbach, Switzerland

^b Bosch Solar Thin Film GmbH, Sonnentor 2, 99098 Erfurt, Germany

ARTICLE INFO

Article history:

Received 7 January 2011

Received in revised form

29 June 2011

Accepted 8 September 2011

Available online 5 October 2011

Keywords:

Microcrystalline silicon

Solar cell

Raman crystalline fraction

ABSTRACT

The performance of micromorph silicon tandem solar cells deposited by plasma enhanced chemical vapor deposition (PECVD) at 40 MHz was investigated in a large area industrially employed reactor as a function of the crystalline fraction of the microcrystalline bottom cell. The relevant plasma parameters frequency, pressure, hydrogen and silane mixture, temperature were kept constant. The RF-power for the deposition of the bottom cell was varied in order to scan its Raman crystalline fraction over the transition region from amorphous into highly crystalline. Assuming constant amorphous or microcrystalline material quality (in terms of stability and defect density) the optimum value of the Raman crystalline fraction and especially the width of the optimum range was thus determined quantitatively. It is shown that the optimum Raman crystalline fraction of the bottom cell on substrates with front contact and amorphous top cell is $52\% \pm 10\%$. A clear decrease of short circuit current density is observed for too high crystalline fraction.

© 2011 Elsevier B.V. All rights reserved.

1. Introduction

The demand for both higher efficiency and lower costs of the thin-film silicon photovoltaic industry leads to the development of a tandem cell concept with an amorphous silicon top cell combined with a microcrystalline silicon bottom cell. This so-called micromorph silicon thin film tandem cell was first introduced by Meier et al. at the Institute for Microtechnology (IMT) at the University of Neuchatel in 1994 [1]. In the last decade, this technology was further improved so that it could be introduced to the photovoltaic industry. The optimum layer quality especially of the actively absorbing intrinsic layer of the microcrystalline bottom cell is strongly depending on the crystalline fraction [2]. This crystalline fraction can be indirectly measured by means of Raman spectrometry, from which the semi-quantitative value of the Raman crystallinity (RC) can be derived. Even though this RC value does not represent the real crystalline fraction it is a well established number which characterizes in a reproducible manner the crystalline fraction of the material. The influence of the Raman crystallinity on the open circuit voltage V_{oc} and the short circuit current density J_{sc} was studied in single junction cells

produced by various techniques like plasma-enhanced chemical vapor deposition (PECVD) [3–5], hot wire chemical vapor deposition [6–8] or microwave plasma [9] showing all similar trends of decreasing V_{oc} with higher Raman crystallinity whereas J_{sc} increases. The microcrystalline process is very sensitive to variations of the process and hardware parameters. Small variations in the plasma conditions can lead to significant deviations in the material quality of the microcrystalline layers. The closer to the transition between amorphous and microcrystalline growth the plasma is operated the more sensitive becomes the process. Especially the perturbation of the plasma edge in the large area reactor behave differently for the two very different deposition regimes for amorphous and microcrystalline silicon layers. Therefore for the development of the reactor toward better uniformity the optimum value and the range of the Raman crystallinity under the conditions prevailing in the real production equipment for micromorph module production. Knowing these target values the required effort to be made for the hardware development can be estimated and eventually limited.

For improving the uniformity generally depositions are made on float glass instead of realistic TCO substrates with an amorphous top-cell on it as it is used in production. It is known that the RC value is influenced by the substrate properties [10], i.e. using bare float glass or commercially available glass substrates coated with transparent conductive oxide (TCO) leads to significantly different RC values. Therefore the correlation must be known between the RC-values on float glass to the RC-values

* Corresponding author. Present address: University of Applied Science, HES-SO Valais, Route du Rawyl 47, CH-1950 Sion, Switzerland. Tel.: +41 27 606 8742; fax: +41 27 606 8815.

E-mail addresses: christoph.ellert@hevs.ch, christoph_ellert@yahoo.com (Ch. Ellert).

on TCO/a-Si cell substrates in order to be able to transfer the development based on float glass to real production conditions.

Since the strong influence of the Raman crystallinity on the cell performance is well established the purpose of this experiment is to determine both the value of the optimum Raman crystallinity under production relevant process conditions and the range within which the RC-value needs to be kept constant over the entire surface of the substrate within the PECVD reactor. In addition, the influence of RC-values deviating from the optimum value on the relevant cell parameters is investigated in this work. In the experiments described in the following only micromorph tandem cells and no single junction cells were deposited and measured.

2. Material and methods

The intention of the experiment was to obtain the dependence of the cell parameters like the conversion efficiency η , open circuit voltage V_{oc} , short circuit current density J_{sc} , and fill factor FF on the Raman crystallinity. The Raman crystallinity can in principle be modified by means of any of the deposition parameters like temperature, radio-frequency (RF) power, total gas flows, silane concentration and pressure. Since we were interested in a variation of RC while varying as little as possible the other layer properties—especially the thickness, we decided to vary the RF-power. This is based on the observation that in the process regime which is predominantly used for microcrystalline layers, the so-called “strongly depleted regime”, the RF-power has a strong impact on RC while relatively little influencing the deposition rate, see Fig. 1.

It can be seen that a variation of RF-power of about 500 W leads to an increase in RC from 0.4 to 0.7, i.e. crossing the entire relevant range for good microcrystalline solar cell material. The same power variation however increases the layer thickness (and thus the deposition rate) by less than 5%.

In order to keep conditions as precisely constant as possible the whole experiment was designed in three steps:

1. *Determination of RF-range and deposition rate:* Six single layers were deposited on float glass at different RF-powers on which we measured thickness and Raman crystallinity, see Fig. 1. From these we could determine the required RF-power values in order to obtain the desired Raman values with the proper

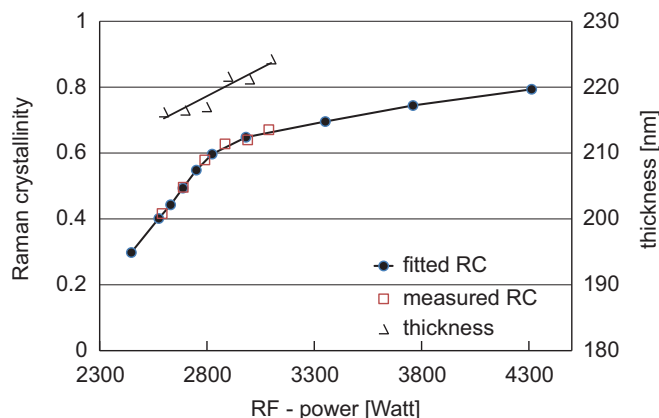


Fig. 1. Increase of the Raman crystallinity and the layer thickness with RF-power measured in the center of single microcrystalline layers on float glass. All depositions were done with the same deposition time. The thickness values were linearly fitted whereas for the measured RC-values a non-linear spline was required. In the transition region from nearly amorphous to mainly microcrystalline material the rate increases by less than 5%.

spacing to cover the full range from very low Raman crystallinities around 30% (i.e. nearly amorphous) to material with high crystallinity fraction around 80%.

Based on the predetermined deposition rate deduced from the results in Fig. 1 the deposition time for the intrinsic absorber layer (i-layer) for the following steps 2 and 3 was corrected in order to obtain a constant i-layer thickness in the microcrystalline bottom cell.

2. *Verification of Raman crystallinity and layer thickness:* A first set of 10 float glasses were coated on a large-area R&D deposition tool with the preselected RF-powers and the corrected deposition times in order to reach the desired film thickness of 1.5 μm . This set was used to verify rate, thickness and proper Raman values for the given tool. Here the thickness was measured using a profilometer.
3. *Cell deposition:* In a second set of 10 depositions eventually commercially available TCO substrates were coated with the parameters as verified in step 2. This last step provided 1 cm^2 cells and $10 \times 10 \text{ cm}^2$ so-called XS modules which are distributed over the entire substrate area of $1100 \times 1300 \text{ mm}^2$. In this second set of depositions all other layers in the entire tandem cell stack were kept constant for all 10 cell depositions. Therefore the only varied parameter was the RF-power during the intrinsic layer and the deposition time, thus leading to the ideal experiment of only modified RC with otherwise entirely identical cell stacks.

Performing step 2 and 3 allows correlating RC values measured on the TCO/top-cell substrate used for bottom cell deposition to the RC-values deposited directly on float glass. This correlation is interesting to obtain because the uniformity of a single layer in a reactor is very often used as a judgement criterion for the quality of the machine. Therefore, it was generally used for the optimization of the uniformity of Raman crystallinity in the large area reactor. However, the uniformity of any layer parameter like rate or RC measured on float glass can deviate from the uniformity measured on the real module substrate, i.e. the top cell on a TCO substrate. For cells the TCO substrates were divided by laser scribing into many test cells, as defined in the pattern shown in Figs. 2 and 3. These micromorph solar cells were cut out from the large area substrates and the photovoltaic performance was measured on the 16×8 cell samples of 1 cm^2 .

The whole experiment was performed twice. Both series were done in a standard Oerlikon PECVD reactor optimized for microcrystalline silicon ($\mu\text{c-Si}$) depositions as it is used in production equipment suitable for large area substrates of $1100 \text{ mm} \times 1300 \text{ mm}$ size. In the first series commercially available SnO_2 substrates were used. The deposition of the microcrystalline layers was done at a RF-frequency of 40 MHz and a plasma gap of 28 mm. The deposition parameters were 6% Silane in H_2 at a pressure of 2.5 mbar and a substrate temperature of 160°C . The deposition rate was thus in the range of 4.27 \AA/s – 4.57 \AA/s . The total bottom cell i-layer thickness was kept near 1450 nm by choosing the adapted deposition time. In addition, pieces of cover glass were placed on the large area TCO/top cell/bottom cell substrate during back contact depositions in order to measure Raman crystallinity directly into the silicon layer stack of the bottom cells. The position of these cover glasses is marked in blue in the layout for the first experiment in Fig. 2.

The second experiment was done on commercially available SnO_2 front contact as well but using a modified PECVD reactor with improved uniformity. Herein the deposition parameters were as well 6% Silane in H_2 mixture but with a 17% increased total gas flow compared to the first experiment. These parameters yield a deposition rate of 5.69 – 6.13 \AA/s using RF-power between 2800 W and 3920 W. The deposition time of the i-layer was chosen such that the i-layer thickness is kept constant for

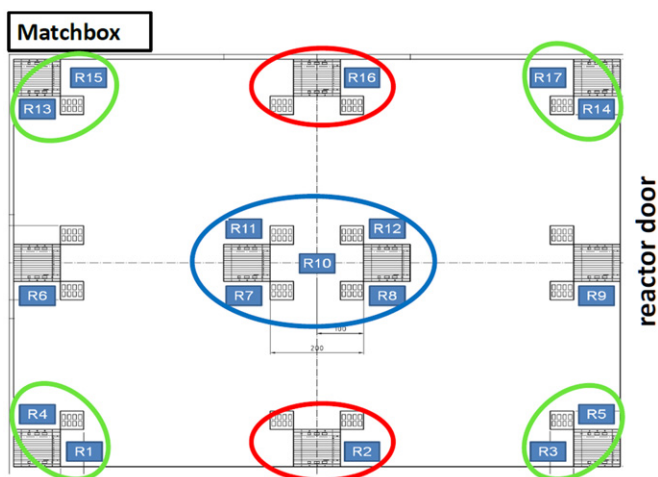


Fig. 2. Distribution of test cells (small gray squares) on the commercial TCO substrate for the first experiment. Each $50 \times 50 \text{ mm}^2$ cell sample consists of eight individual test cells of 1 cm^2 . At the 17 blue positions (numbered Rx with $x = 1-17$) a thin cover glass was positioned during the deposition of the back contact, in order to have access to the silicon layer stack for the Raman measurements geometrically close to the cells. Cell performance data as well as Raman crystallinity values for this first experiment were obtained by averaging over all samples within the regions marked with three colored elliptical shapes respectively. The larger gray squares are $10 \times 10 \text{ cm}^2$ modules. The entrance door to the reactor was situated on the right end of this figure. (For interpretation of the references to color in this figure legend, the reader is referred to the web version of this article.)

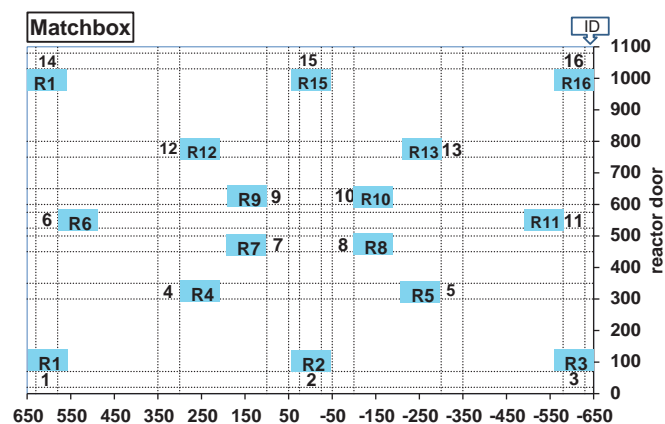


Fig. 3. Distribution of test cells (small white squares, numbered from 1 to 16) on the large area TCO substrate for the second experiment. The entrance door to the reactor was situated on the right end of this figure, i.e. close to samples 16, 11 and 3. At the blue positions (numbered Rx with $x = 1-16$) samples were cut in order to measure the Raman crystallinity for correlation to the cell performance. The distance along the long and short edge are given in millimeters. The view is shown from the layer side on the substrate. (For interpretation of the references to color in this figure legend, the reader is referred to the web version of this article.)

all 10 layers at 1500 nm . The Raman measurement was done through the back contact ZnO which is transparent for the 514 nm Argon laser of the Raman spectrometer. Therefore covering the substrate on specific positions during back contact depositions was considered unnecessary in the second experiment.

Since the uniformity of RC in the reactor is not perfectly flat the RF-power for the deposition was determined for the center of the substrate as point of reference. In both experimental series, the order of the 10 depositions with different RF-power was irregularly chosen on purpose such that potential drifts of any parameter could be excluded, i.e. neither in increasing nor decreasing the order of power values but mixed.

The thickness was measured by spectroscopic ellipsometry using the AccuMap M-2000 UV with NIR extended range by J. A. Woollam.

The angle of incidence was fixed at 65° . A Generalized-Oscillator model was used to fit the interference pattern in the spectra of the two measured reflection coefficients for perpendicular and parallel polarization, respectively. The layer stack was modeled as follows: Cauchy oscillator for the float glass substrate and Tauc-Lorentz oscillators for the microcrystalline silicon i-layer. Finally to approximate the roughness of the surface of the sample the effective media approximation (EMA) was used as common with 50% of silicon material and 50% voids. The thickness of the adhesion layer and its effect on the ellipsometry data was neglected. Note that the measurement of layer thickness by ellipsometry requires flat substrates in order to obtain reliable data, i.e. rough TCO which is optimum for good cell performance is not suitable.

The Raman measurements were done with a commercially available Raman spectrometer, Renishaw InVia Reflex at the 514 nm Argon laser line. Light is perpendicularly incident from the layer side, the backscattered Raman signal separated via Notch filters from the incident light, diffracted by a grating and recorded on a Peltier cooled linear CCD array as a function of the Raman shift, see an example in Fig. 4.

For obtaining reproducible Raman crystallinity values it is essential to keep a very precise fitting routine. Briefly this includes fixing upper and lower fitting limits for the center of the three peaks, which are commonly described as the amorphous phase (a-Si) at 480 cm^{-1} , the crystalline phase (c-Si) around 520 cm^{-1} and the so-called defective crystalline phase near 510 cm^{-1} which is sometimes called mixed crystallinity peak (mc-Si). In addition a linear background was taken into account. Note that the estimated thickness of the cells is usually by far more than $1 \mu\text{m}$, whereas the Raman collection or information depth of the green light into the silicon layer is only about 50 nm for a-Si:H and 120 nm to 170 nm for the microcrystalline phase [11]. Since the Raman scattered light must travel across the same thickness of material again before reaching the detector, this information depth of the Raman measurement is half of the penetration depth. The fitted surface area of the each peak is interpreted as the intensity of the corresponding oscillation. From these one obtains the so-called Raman crystallinity fraction

$$RC = \frac{I_{mc-Si} + I_{c-Si}}{I_{a-Si} + I_{mc-Si} + I_{c-Si}} \quad (1)$$

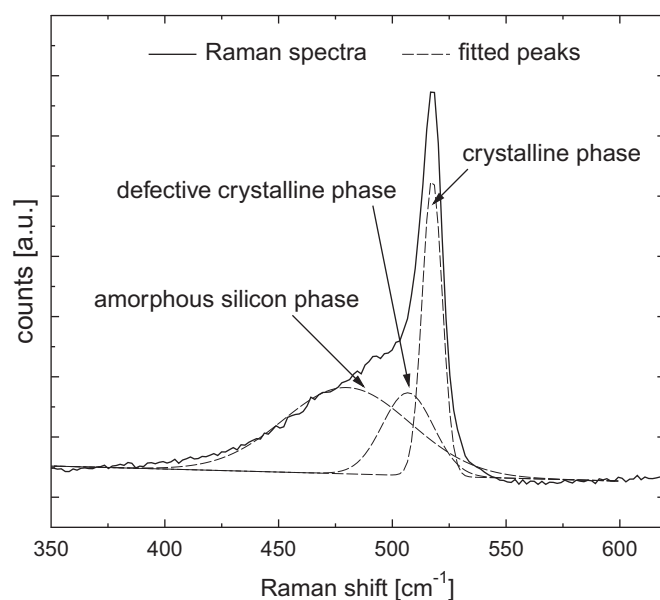


Fig. 4. Typical spectrum obtained with the commercial Raman spectrometer showing the measured (solid line) scattering feature of a microcrystalline sample to which three peaks can be fitted (dashed line), see Ref. [4].

Note that this Raman crystalline fraction does not represent the real volume fraction of crystalline material inside the entire volume of the microcrystalline layer. It is however widely accepted in the silicon thin film community as a representative and reproducible measure of the amorphous to crystalline ratio which strongly influences the cell performance. This Raman measurement method was identically performed on the first set of 10 depositions on float glass as well as on the micromorph tandem cells on TCO.

3. Results

The short circuit current density and the conversion efficiency of the cells from the first experimental series are shown in Fig. 5 as a function of the Raman crystallinity measured on the TCO substrate. Three data series are shown, which were taken as an average of the three typical regions according to the layout in Fig. 2. The four corners, the middle position of the two long edges and the four cell samples in the center of the large substrate. The strong scattering of data points is explained by the fact that measurement of RC on TCO glass and of cell properties were not done on exactly the same position. Therefore a point can move quite a bit in the diagram. This figure shows a first trend of the evolution of cell performance with RC.

In the following the results of the second experimental series are presented. The measurement of RC on both float glass and on TCO allows us to correlate these quantitatively, see Fig. 6. It can clearly be seen that RC on TCO is about 5–8% (absolute RC) lower

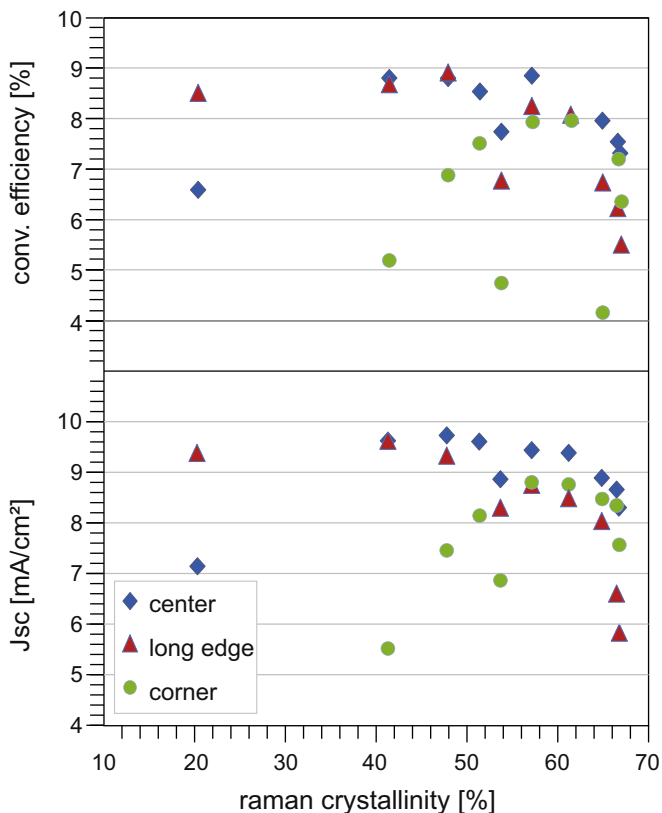


Fig. 5. Dependence of the conversion efficiency and the short circuit current density J_{sc} on the Raman crystallinity from the first experimental series, according to the layout in Fig. 2. The relatively low values of J_{sc} are due to the application of a simplified dielectric back reflector in the experiments in order to both reduce the experimental efforts and pronounce the bottom cell current limitation.

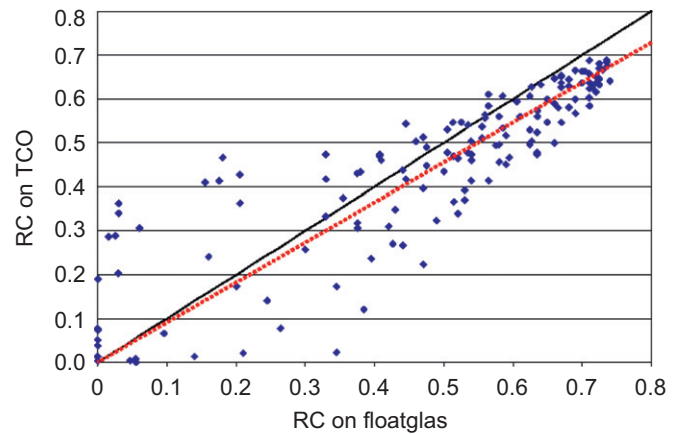


Fig. 6. Correlation of the Raman crystallinity measured on front contact TCO and top cell as a function of RC on float glass always at the same position inside the reactor.

than on float glass. This Raman shift might be described by a linear function through the origin, a more detailed dependence may not be attributed due to the strong scattering of the data points. The properties of the substrate play a significant role for nucleation and the structure of the growing film, as is shown in [10] and [12], therefore a modification of growth conditions can easily be imagined.

In Fig. 7 the relevant cell parameters are plotted as function of the Raman crystallinity on TCO glass. The conversion efficiency shows a maximum at RC around 55%, dropping slightly more sharply toward higher than toward lower crystallinity. The open circuit voltage V_{oc} drops nearly linearly with increasing crystallinity, as it is known from previous publications, for example [8]. The short circuit current density J_{sc} increases with increasing RC up to about 50% before it drops sharply for RC above 60%. Finally the fill factor FF is nearly constant between $RC \approx 20\%$ and $RC \approx 65\%$. Above this range of RC the strong mismatch between the top and bottom cell currents results in an increase of FF . Thus the maximum in conversion efficiency is mostly due to the behavior of the current density J_{sc} , however shifted to lower values due to the dropping open circuit voltage.

4. Discussion

As was shown in the literature the Raman crystallinity plays a crucial role for the cell performance of micromorph silicon tandem cells. In these two experimental series we demonstrate this dependence on this parameter with as little as possible changing thickness, rate or other parameters. From the first experimental series it became obvious that the optimum RC is clearly below 70%, see Fig. 5. It can be seen that the main reason for this optimum lies in the maximum of the current density. From the second experimental series, shown in Fig. 7, the optimum RC for highest J_{sc} in cells is near 45% to 50% with an uncertainty range of around 10%. The open circuit voltage V_{oc} decreases over the whole range with increasing RC. This is due to the band gap which decreases with increasing crystallinity. The fill factor however is nearly constant over a large range from RC 25% to 75%. The current density J_{sc} reaches its highest value between 45% and 65% decreasing on both sides toward higher as well as lower RC. For lower RC this decrease can be explained by the lower absorption coefficient of more amorphous phase material in the red wavelength range. For higher RC however the decreasing current density is unexpected since the absorption

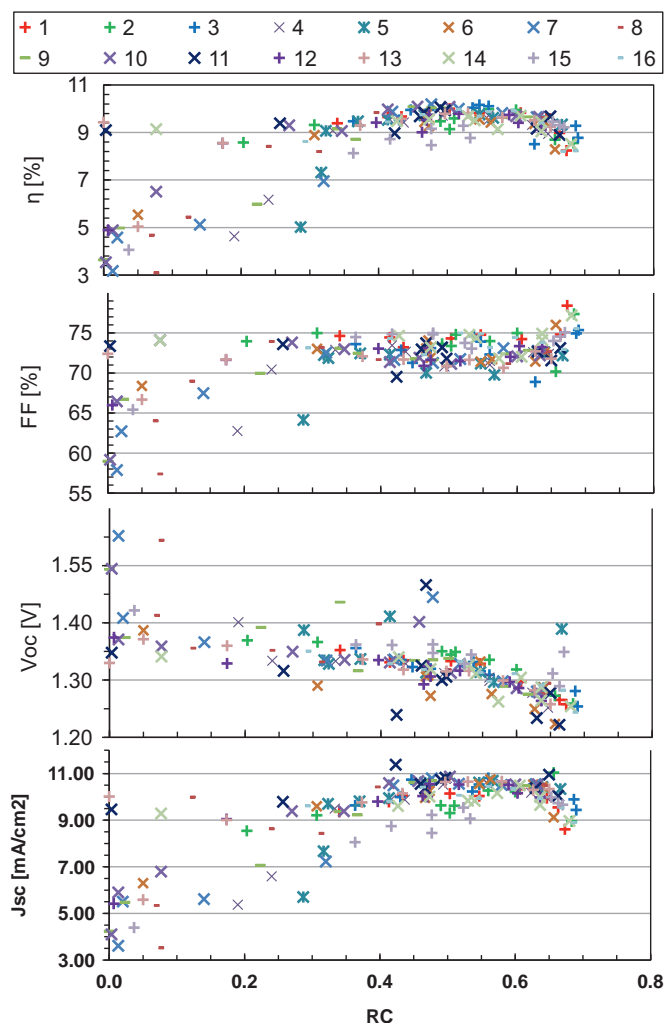


Fig. 7. Dependence of the conversion efficiency η , the fill factor FF , the open circuit voltage V_{oc} and the short circuit current density J_{sc} on the Raman crystallinity. The relatively low values of J_{sc} are due to the application of a simplified dielectric back reflector in the experiments in order to both reduce the experimental efforts and pronounce the bottom cell current limitation.

coefficient becomes larger in the red wavelength range. Possibly, the defect density is increasing with the higher crystalline fraction resulting in a higher recombination rate. A potential source of defects is the existence of nanosized cracks in the i-layer material [13] which should be subject of further research.

In the first experiment (Fig. 5) the three series differ more between each other as they differ compared to the second experiment (Fig. 7). Especially the green circles drop much more quickly for decreasing RC values than the others. We attribute this observation to the fact that the first experiment was performed in a previous generation PECVD reactor, since it was done more than half a year earlier than the second experiment. This older reactor type has less good uniformity of plasma conditions than the reactor used in the second experiment. This development of the reactor toward better uniformity was the main motivation for starting this type of experiments (see Section 1). Especially the four reactor corners (green circles) showed strong variations in the Raman crystallinity across very short distances of a few centimeters only.

In this study, we showed that together with the decrease of V_{oc} with RC the maximum in J_{sc} leads to the slightly lower optimum in RC for the conversion efficiency. The decrease of the conversion efficiency toward lower and higher crystallinity values is mainly

due to an optimum in current density near 60% superposed by an increase in V_{oc} with decreasing RC.

One potential source of error is that the Raman crystallinity was not measured exactly on the cells themselves but about 5 cm shifted sideways as described in Figs. 2 and 3. Especially at the edges of the reactor the RC value can vary strongly even over few centimeters. Therefore we estimate this to be the main cause of the strong fluctuations in the Figs. 5 and 7. The Raman measurement of the second experiment was performed through the back contact TCO. However, since the TCO is transparent for the laser wavelength used for the Raman measurement we do not expect an influence of the TCO on our results. The amorphous n-layer which covers the microcrystalline i-layer is about 20 nm thin which is half of the Raman information depth for amorphous layers. Since the uniformity of the n-layer thickness is better than $\pm 10\%$ the influence of this non-uniformity on our results is estimated to be smaller than 5%.

Note that the Raman measurement as described above probes less than the upper 200 nm of the about 1.5 μm thick microcrystalline i-layer of the bottom cell. Vertical variations in RC in different places of the reactor are therefore not detectable here. However, it can easily be imagined that these effects start to play a role as soon as the uniformity of the plasma deposition conditions improves and reaches low values of a few percent only. These effects of vertical variations in RC and methods to actively control it by varying the H_2 -dilution during the process (as shown in [14]) are presently actively pursued topics of research and development.

5. Conclusion

This experiment using large-area close-to-production deposition equipment yielded quantitatively the influence of the Raman crystallinity of the microcrystalline bottom cell on the relevant cell parameters of thin film micromorph silicon tandem modules, i.e. conversion efficiency η , open circuit voltage V_{oc} , short circuit current density J_{sc} and fill factor FF . Furthermore, it was shown that the Raman crystallinity measured on float glass is higher than the measured value in the absorber layer of the micromorph cell stack, which is deposited on the rough TCO substrate and includes the doped n-layer. The optimum of RC on commercial SnO_2 TCO substrates is shown to be between 45% and 55%. Therefore for optimum performance of large area modules the uniformity of the Raman crystallinity of the deposited microcrystalline i-layer over the full area of large modules must be kept within a band of $\pm 10\%$. Further PECVD process and hardware development should be directed to enable homogeneous depositions of compact microcrystalline i-layers within the optimum RC range on large areas and with high deposition rate.

Acknowledgments

The authors are grateful to Nadja Schrader, Oerlikon Solar, who performed the Raman measurements during the preparation as well as final evaluation phase of the experiments as well as Nadya Oeftger and Nick Helms, Bosch Solar Thin Film, for the depositions, sample preparation and measurements of the photovoltaic performance.

References

- [1] J. Meier, S. Dubail, R. Flückiger, D. Fischer, H. Keppner, A. Shah, Intrinsic microcrystalline silicon ($\mu\text{c-Si:H}$) - a promising new thin film solar cell material, in: Proceedings of the First WCPEC, vol. 1, Hawaii, USA, 1994, pp. 409–412.

- [2] O. Vetterl, F. Finger, R. Carius, P. Hapke, L. Houben, O. Kluth, A. Lambertz, A. Mück, B. Rech, H. Wagner, Intrinsic microcrystalline silicon: a new material for photovoltaics, *Solar Energy Materials and Solar Cells* 62 (2000) 97–108.
- [3] M. Kondo, Microcrystalline materials and cells deposited by RF glow discharge, *Solar Energy Materials and Solar Cells* 78 (2003) 543–566.
- [4] C. Droz, E. Vallat-Sauvain, J. Bailat, L. Feitknecht, J. Meier, A. Shah, Relationship between Raman crystallinity and open-circuit voltage in microcrystalline silicon solar cells, *Solar Energy Materials and Solar Cells* 81 (2004) 61–71.
- [5] S. Klein, T. Repmann, T. Brammer, Microcrystalline silicon films and solar cells deposited by PECVD and HWCVD, *Solar Energy* 77 (2004) 893–908.
- [6] Y. Mai, S. Klein, R. Carius, H. Stiebig, X. Geng, F. Finger, Open circuit voltage improvement of high-deposition-rate microcrystalline silicon solar cells by hot wire interface layers, *Applied Physics Letters* 87 (2005) 073503.
- [7] S. Klein, F. Finger, R. Carius, M. Stutzmann, Deposition of microcrystalline silicon prepared by hot-wire chemical-vapor deposition: the influence of the deposition parameters on the material properties and solar cell performance, *Journal of Applied Physics* 98 (2005) 024905.
- [8] Y. Wang, X. Geng, H. Stiebig, F. Finger, Stability of microcrystalline silicon solar cells with HWCVD buffer layer, *Thin Solid Films* 516 (2008) 733–735.
- [9] G. Ohkawara, M. Nakajima, H. Ueyama, H. Shirai, Relationship between microstructure and photovoltaic performance in microcrystalline silicon film solar cells fabricated by a high-density microwave plasma, *Thin Solid Films* 427 (1–2) (2003) 27–32.
- [10] E. Vallat-Sauvain, J. Bailat, J. Meier, X. Niquille, U. Kroll, A. Shah, Influence of the substrate's surface morphology and chemical nature on the nucleation and growth of microcrystalline silicon, *Thin Solid Films* 485 (2005) 77–81.
- [11] C. Droz, *Thin Film Microcrystalline Silicon Layers and Solar Cells: Microstructure and Electrical Performances*, PhD Thesis, University of Neuchatel, IMT, 2003.
- [12] M. Python, O. Madani, D. Dominé, F. Meillaud, E. Vallat-Sauvain, C. Ballif, Influence of the substrate geometrical parameters on microcrystalline silicon growth for thin-film solar cells, *Solar Energy Materials and Solar Cells* 93 (2009) 1714–1720.
- [13] M. Python, E. Vallat-Sauvain, J. Bailat, D. Dominé, L. Fesquet, A. Shah, C. Ballif, Relation between substrate surface morphology and microcrystalline silicon solar cell performance, *Journal of Non-crystalline Solids* 354 (2008) 2258–2262.
- [14] M.N. van den Donker, T. Kilper, D. Grunsky, B. Rech, L. Houben, W.M.M. Kessels, M.C.M. van de Sanden, Microcrystalline silicon deposition: process stability and process control, *Thin Solid Films* 515 (2007) 7455–7459.